ISSN: 2716-9227 Algerian Journal of Engineering and Technology 08 (2023) 212–219 e-ISSN: 2716-9278

Algerian Journal of Engineering and Technology

Journal homepage: https://jetjournal.org/index.php/ajet

Original Article

Modeling of nuclear reactor core for power control simulation with temperature feedback and xenon concentration effect

Bélaid Djaroum[a]*, Boussaad Mohammedi[a], Abderrahmane khelil. Khelil[b], Sofiane Laouar[a]

[a]*Nuclear Technology Division, Nuclear Research Center of Birine, Djelfa, Algeria*
[b]*Reactor Division, Nuclear Research Center of Birine, Djelfa, Algeria*

ARTICLE INFO

Article history:
Received 27 June 2023
Revised 04 November 2023
Accepted 11 November 2023

Keywords:
Modeling;
Nuclear reactor;
Power control;
PID;
Python Algorithms.

ABSTRACT

Modeling nuclear reactor cores stands as an essential initial step in nuclear technology research and development. The reactor core, serving as the primary thermal energy source in nuclear power plants (NPPs), plays a pivotal role. Such reactor core modeling serves various objectives, including core power control and load-following operations within NPPs. In this study, the pressurized water reactor (PWR) core was modeled using the point reactor method, a technique widely applied in conjunction with multiple reactor core power control strategies during load-following operations. Employing a proportional-integral-derivative (PID) controller, load-following scenarios tailored to grid load maneuvers were implemented in the developed reactor core model. The study also delved into the effects of temperature feedback and xenon. The analysis of simulation results revealed only a very small deviation in power between the desired and actual reactor core power. A substantial movement of the control rods effectively countered the notable impact of xenon on reactor power. Regarding temperature feedback, its contribution to the core total réactivity with a negative reactivity was confirmed. This study utilized the Python language for both the development of the nuclear reactor model and the creation of algorithms required for power control during load-following mode. Typically, similar endeavors with distinct objectives are conducted using MATLAB SIMULINK.

1. Introduction

A nuclear reactor is a complex, nonlinear, and time-varying system [1]. Consequently, controlling the power within the reactor core proves to be a challenging task. Ensuring the safe operation of nuclear reactors requires precise control of core reactor parameters, including thermal power, coolant and fuel temperature, as well as power axial offset—making it a formidable endeavor in nuclear reactors. The load-following mode for nuclear reactors is mainly performed to control the core power and the axial offset simultaneously [2, 3]. Consequently, over the decades, continuous work has been devoted to the research including modeling nuclear reactor cores, stability, and load-following control for reactor cores. Up to now, there exists a set of nuclear reactor core modeling approaches for different purposes. In the point nuclear reactor core modeling method, the core is regarded as a point without any space profile, the parameters core only varies with time [4, 5]. This method was widely applied to the power control of NPPs using several advanced methods and to analyze the stability of the PWR core related to power transients caused by xenon transients during reactor operation in load-following mode [2]. Using this modeling method, the applicability of the second-order sliding-mode control scheme in a nuclear reactor power control and regulation is demonstrated [6]. For the dynamic simulation of the operation of the high-temperature next-generation nuclear reactor, this modeling method is also developed and applied successfully [7]. An application of the point

**Corresponding author*.
E-mail address: b.djaroum@crnb.dz
Peer review under responsibility of University of El Oued.
 https:/dx.doi.org/10.57056/ajet.v8i2.125

kinetics equation with temperature feedback in a nuclear reactor is described and investigated using MATLAB-Simulink Toolbox [8, 9, and 10]. In the present work, modeling of the pressurized water reactor (PWR) core was performed using the point reactor method. By using a proportional-integral-derivative (PID) controller, a scenario of load-following operation, according to load maneuvers on electrical grids, was implemented in the developed reactor core model. The temperature feedback and xenon effect were investigated.

2. Nuclear Reactor Model

This study focuses on the development of a model for the nuclear reactor core, utilizing point kinetics equations. The model incorporates one delayed neutron group of precursors and accounts for feedback from fuel and coolant temperatures [11, 12, 13, 14, and 15]. The influence of the poison (xenon) is also integrated into the reactor model [1, 6, 16]. Regarding the xenon effect, it's important to note that among the fission products present in the reactor core, xenon-135 and samarium-149 (both considered poisons) possess notably large absorption cross sections, resulting in a significant impact on the total reactor core reactivity.

As a result, the developed mathematical model representing the PWR core is organized into four distinct sub-models: the neutronic model, the thermal-hydraulics model, the xenon model, and the external reactivity control model (involving the withdrawal or insertion of control rods). To explicitly outline the function fulfilled by each of these sub-models, the differential equations representing their parameter variations are individually listed below:

2.1. Relative power kinetic sub-model equations

The summary of the point kinetics equations, incorporating six groups of delayed neutrons, is provided below:

$$\frac{dn}{dt} = \frac{\rho(t)-\beta}{\Lambda} n(t) + \sum_{1}^{6} \lambda_i c_i(t) \quad (1$$

$$\frac{dc_i}{dt} = \frac{\beta_i}{\Lambda} n(t) - \lambda_i c_i(t) \qquad i = 1,....,6 \quad (2$$

The application of one delayed neutron group instead of six groups does not compromise the integrity of the core reactor model [6]. By introducing the concept of relative power, the kinetic sub-model can be expressed through the following equations:

$$\frac{dn_r}{dt} = \frac{\rho(t)-\beta}{\Lambda} n_r(t) + \frac{\beta}{\Lambda} c_r(t) \quad (3$$

$$\frac{dc_r}{dt} = \lambda n_r(t) - \lambda c_r(t) \quad (4$$

2.2. Fuel and coolant sub-model equations

$$\frac{dT_f}{dt} = \frac{1}{\mu_f}\left[f_f P_0 n_r(t) - \Omega\left(T_f - T_c\right)\right] \quad (5$$

$$\frac{dT_c}{dt} = \frac{1}{\mu_c}\left[\left(1-f_f\right)P_0 n_r(t) + \Omega\left(T_f - T_c\right) - M\left(T_l - T_e\right)\right] (6$$

2.3. Xenon and iodine sub-model equations

$$\frac{dX}{dt} = \left(\gamma_X \Sigma_f - \sigma_X X\right)\phi - \lambda_X X + \lambda_I I \quad (7$$

$$\frac{dI}{dt} = \gamma_I \Sigma_f \phi - \lambda_I I \quad (8$$

2.4. Total Reactivity sub-model equation

$$\rho_t = \rho_{rod} + \alpha_f\left(T_f - T_{f_0}\right) + \alpha_c\left(T_c - T_{c_0}\right) - \frac{\sigma_X}{\upsilon\Sigma_f}\left(X - X_0\right) \quad (9$$

$$\frac{d\rho_{rod}}{dt} = G_r Z_r \quad (10$$

$$P(t) = P_0 n_r(t) \quad (11$$

Table 1 provides the nomenclature for the parameters and constants found in the differential equations (1-11).

Table 1: Nomenclature

Symbol	Definition
n	Reactor neutron density [n/cm^3]:
c	Reactor precursor density [atom/cm^3]:
n_r	Relative reactor neutron density:
c_r	Relative reactor precursor density:
ρ	Total reactivity in reactor core [pcm]:
β	Total delayed neutron fraction;
Λ	Effective prompt neutron lifetime[s];
λ	Radioactive decay constant [s^{-1}];
T_f	Average reactor fuel temperature [°C];
μ_f	Total heat capacity of the fuel [MW. s/°C];
f_f	Fraction of reactor power deposited in the fuel;
P_0	Initial equilibrium power [MW];
Ω	Heat transfer coefficient between fuel and coolant [MW. s/°C];
Tc	Average reactor coolant temperature [°C];
μ_c	Total heat capacity of coolant [MW. s/°C];
M	Mass flow rate multiply by the heat capacity of the coolant [MW. s/°C];

T_l	The temperature of the water leaving the reactor core [°C];
T_e	The temperature of the water entering the reactor core [°C];
γ_X	Xenon yield by fission
γ_I	Iodine yield by fission
λ_X	Xenon decay constant [s^{-1}]
λ_I	Iodine decay constant [s^{-1}]
α_f	Coolant temperature reactivity coefficient [Δk/k/°C]
α_c	Fuel temperature reactivity coefficient [Δk/k/°C]
T_{f0}	Initial equilibrium fuel temperature [°C]
T_{c0}	Initial equilibrium coolant temperature [°C]
σ_x	Microscopic absorption cross-section of xenon [cm^2]
$\delta\rho_r$	Reactivity due to control rod [Δk/k]
Z_r	Control rod speed [cm/s] or [%/s]
G_r	Total reactivity worth of control rod [pcm]
υ	Average number of neutrons production per fission

The developed model, represented by equations (1-9), is linearized around equilibrium point (n_0, c_0). Using the small perturbation assumptions [1], the resulting linearized model takes the following form::

$$\begin{cases} \dot{x} = \hat{A}\vec{x}(t) + \hat{B}\vec{u}(t) \\ \vec{y} = \hat{C}\vec{x}(t) \end{cases} \quad (12$$

Where $\vec{x}(t) \in R^n$ is the state vector of the model, $A \in R^{n \cdot n}$ is state matrix, $\vec{u}(t) \in R^m$ is the control input vector of the model, $\vec{y}$ is the output vector of the model, $C \in R^{n \cdot 1}$ is the input matrix. These vectors are given as follows, as for the matrices, see reference [1] for more details:

$$x = \left[\delta n_r, \delta c_r, \delta T_f, \delta T_c, \delta X, \delta I, \delta\rho\right]^T$$

$$y = \left[\delta n_r\right],\ u = \left[Z_r\right]$$

In creating the nuclear reactor model, the functions for the Python algorithms, namely Math_Reactor_Model, Reactor_Pow_Reg, Test_Reactor_Model, and Integral_Rod_worth_calculation, are formulated using the differential equations (1-11). To assess the reactor model under load-following conditions, a representative power reactor example is selected [1]. The reactor parameter values utilized in this study are detailed in Table 2.

3. Reactor Power Control Strategy

The power control in a Pressurized Water Reactor (PWR) primarily relies on two control measures: adjusting control rods and altering the concentration of boric acid in the coolant. In this study, only the first control measure is employed for reactor power control. The nuclear reactor core modeling established here overlooks the dynamic iodine-xenon process. Consequently, the power control system analysis is conducted over relatively short timeframes, typically spanning hundreds or thousands of seconds. However, when considering the dynamic iodine-xenon process in reactor core modeling, power control proves suitable for dynamic process analyses spanning longer durations, such as several hours or days. This latter modeling case is the focus of examination in this work.

Furthermore, various control strategies are devised based on a controller employing one of several reactor core power control methods: PID control, feedback control with a state observer, optimal control, neural network control, fuzzy control, model predictive control, H robust control, sliding mode control, and fractional order control [17, 18, 19, and 20]. Among these methods, it is widely recognized that the PID controller stands out as the simplest to design and implement in industrial applications as real-time controllers [1, 21, 22, and 23]. Additionally, the PID controller exhibits reduced overshoot and settling time when compared to a PI controller.

The reactor control strategy diagram included PID controller is schown in Fig.1.

The standard form of a PID controller, described in the time domain, can be articulated by the following equation:

$$u(t) = K_P e(t) + K_I \int_0^t e(\tau) d\tau + K_D \frac{de(t)}{dt} \quad (13$$

Where $K_P, K_I, K_D \in R$ the proportional, integral, and derivative gains, respectively; *e(t)*: error signal; *u(t)* is the model input signal (control action); P_{set}(t) is the desired power to be established in the reactor. *y(t)* is the model output signal, P_{out} is the controlled power of the reactor. The derivative action time constant $(\tau > 0)$ is assumed to be fixed.

Table 2: Reactor parameter values, in 100% of nominal power

Parameter	Value
Thermal power	2500MW
Core heights	400cm
Core radius	200cm
Diffusion constant (D)	0.16cm
Mean velocity of neutrons (v)	2200m/s
Microscopic absorption cross-section (σ_x)	$3x10^{-18}$ cm2
Fractional fission yield of Xenon (γ_x)	0.003
Fractional fission yield of Iodine (γ_I)	0.059
Xenon decay constant (λ_x)	

Iodine decay constant (λ_I)	2.1x10-5s-1
Macroscopic fission cross-section (Σ_f)	2.9x10-5s-1 0.3358cm^{-1}
Total delayed neutron fraction (β)	0.0065
Total reactivity worth of rod	0.145pcm
Total heat capacity of the fuel (μ_f)	26.3MW.s/°C
Total heat capacity of the coolant (μ_c)	71.8MW.s/°C
Effective prompt neutron lifetime (Λ)	2x10-5s
Fraction of reactor power deposited in the fuel (f_f)	0.92

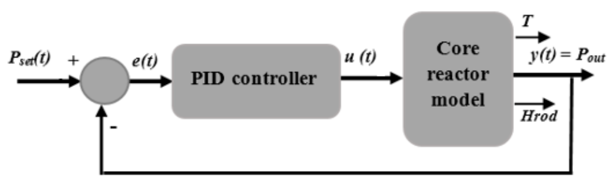

Fig 1. Reactor core power control strategy with PID controller.

3.1. Control rod and worth calculation algorithm

In this study, the control strategy for adjusting reactor power is exclusively based on the external manipulation of control rods. To accommodate this approach, an algorithm is devised to calculate the reactivity worth of control rods, considering their prescribed step movement limit [24, 25, and 26]. Equation (10), representing the deviation in external reactivity, serves as the foundation for this Python algorithm. In addition to determining the total worth reactivity of the control rods (denoted as Gr in the same equation), it is crucial to select the speed at which they are moved. For example, a fixed speed of 2 cm/s and a displacement height of 386 cm are chosen, values specified in the characteristic table of the VVER-1200 reactor control rod mechanism. Typically, the relationship between reactivity and rod position can be empirically determined. However, for PWR reactors, an approximate polynomial function, obtained through mathematical software, is suggested for calculating the integral efficiency of any control rod, assuming a constant reactivity coefficient. The proposed polynomial expression is provided below:

$$y(h) = \left(\frac{0.00175}{4} h^4 - \frac{0.3675}{3} h^3 + \frac{19.45}{2} h^2 \right) \times \rho_{scaling} \qquad (14$$

Where: h is the control rod position [%] inserted in core reactor; $\rho_{scaling}$ is the reactivity-scaling factor.

As an example, consider one of the 12 control rod groups of the VVER-1200 reactor, specifically group №10. When completely inserted (h = 0%) into the core reactor, it introduces a negative reactivity of 1302.59 pcm. Utilizing the developed Python algorithm to simulate reactivity insertion steps for control rod groups with ρscaling = 0.07041 pcm, the resulting data is illustrated in Fig. 2.

Taking into account the two characteristics of the VVER-1200 control rod mechanism, when moving group №10, the maximum step reactivity insertion is 6,7491 pcm per second.

In Fig. 2, the curve is divided into three segments: a linear section between 20% and 60%, and two non-linear sections between 0% and 20%, and 60% and 100%, respectively. The linear part of control rod insertion/extraction is employed for reactor power regulation. Additionally, it is evident from this curve that at a 20% withdrawal of rod group №10, the integral rod worth is 209.82 pcm; at 40%, it is 622.42 pcm; at 80%, it is 1227.95 pcm, and at 100% withdrawal, the integral rod worth is 1302.59 pcm [27, 28].

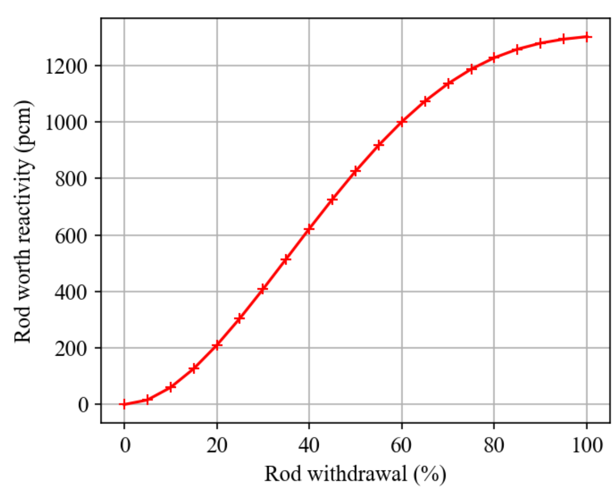

Fig 2. VVE-1200 integral control rod worth of group №10.

4. Results and Discussion

To evaluate the developed reactor model, accounting for temperature feedback and considering the impact of xenon on total reactivity in the reactor core, a load-following mode operation scenario is proposed. The scenario spans a duration of 12 hours: the reactor reaches its nominal power and maintains it for the first three hours. Subsequently, power reduction commences and continues until reaching 60% after 2 hours. This power level is sustained for 4 hours, so after 9 hours from the initiation of the scenario, there is an increment in power until it reaches the reactor's nominal power after an additional 2 hours. The nominal power is then maintained during the final hour of the cycle. The simulation time step is set at 0.1 seconds, and the desired power is expressed as a percentage of the reactor's nominal power. The vectors for desired power and simulation time, along with the PID parameters, are provided as follows:

- $t_{sim} = \left[0, \ 3, \ 5, \ 9, \ 11, \ 12\right] * 3600$
- $P_{desired} = \left[100, \ 100, \ 60, \ 60, \ 100, \ 100\right]$
- $[K_P, K_I, K_D]$ = [13.8005, 0.3285, 0.0036]

The simulation results from the developed model are presented in two scenarios: one without considering the xenon effect (WOXE) and the other accounting for xenon effect (WXE) on the total reactivity in the reactor core. These results are visualized in Figures (3, 4, 5, 6, 7, and 8).

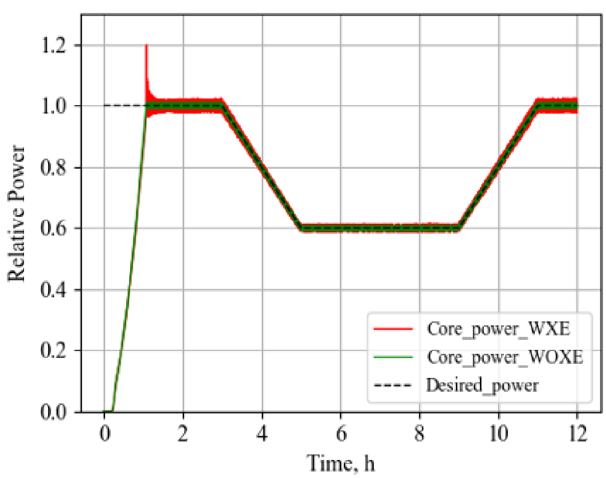

Fig 3. Power variation with PID controller [100%-60%-100%].

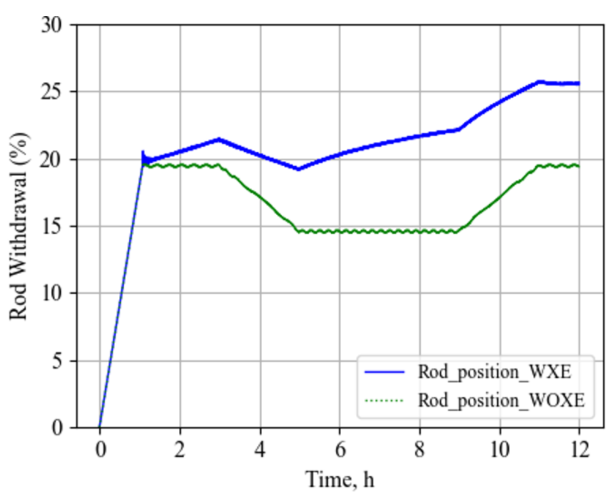

Fig 4. Rod withdrawal from reactor core bottom.

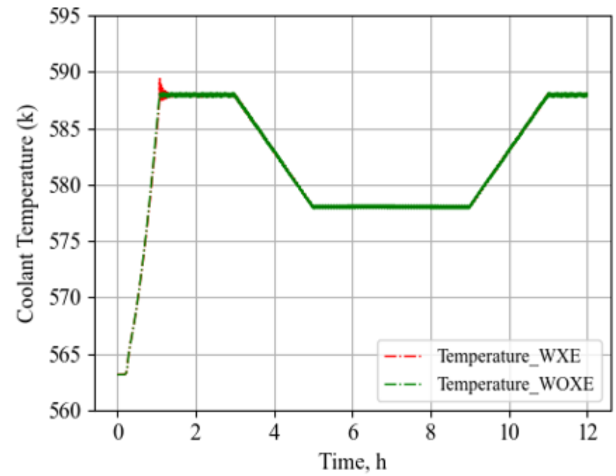

Fig 5. Coolant temperature variation.

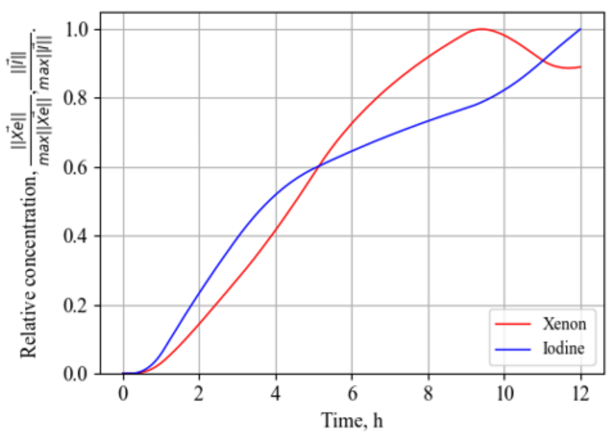

Fig 6. Xenon and Iodine relative concentration.

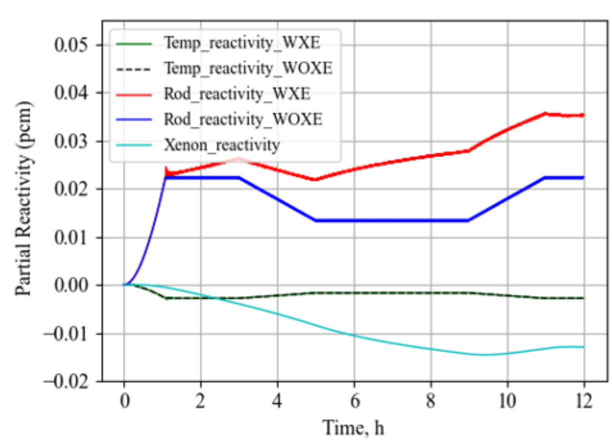

Fig 7. Partial reactivity due to rod movement, coolant temperature, and xenon.

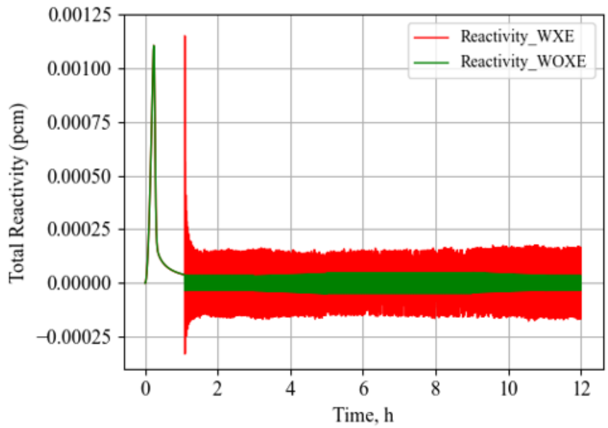

Fig 8. Total reactivity in reactor core (unfiltered signal).

Upon analyzing and processing the total reactivity signal result, depicted in Fig. 8, the application of filters enables the extraction of valuable insights regarding the total reactivity parameter within the reactor core. This extraction aims to scrutinize the dynamic behavior of the reactor core in response to various influences, such as temperature feedback and xenon. The outcome of this processing is displayed in Fig. 9.

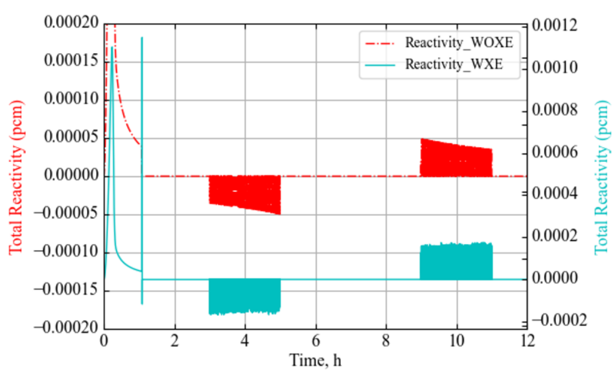

Fig 9. Total reactivity in reactor core (filtered signal).

The simulation results are carefully examined to gain insights into the responses of the core reactor model (output parameters) and to assess the effectiveness of the power control strategy. In Fig. 3, it is observed that the relative reactor power, first without considering the xenon effect on total reactivity (WOXE) and then with its influence, shows a negligible deviation from the desired power in the absence of xenon effect. However, in the presence of xenon effect (WXE), there is a more significant deviation before the model stabilizes, indicating that the xenon effect widens the band of power regulation. Nevertheless, the proposed power control strategy utilizing a PID-Controller for monitoring reactor core power demonstrates good agreement with the desired power.

Furthermore, Fig. 4 illustrates that the adjustment of control rods becomes more critical for power control in the presence of xenon effect. This allows for compensation of the negative reactivity introduced by xenon, ensuring a minimal deviation between reactor power and the desired level, especially at a sustained relative power level (60%) over 4 hours.

The curve representing the variation in coolant temperature in Fig.5 shows that these fluctuations are a consequence of changing power levels. The feedback effect is effectively managed by making minor adjustments to the position of the control rods. Additionally, the negative feedback from the refrigerant is confirmed by the partial reactivity curve associated with the refrigerant temperature, as depicted in Fig.7.

The dynamics of xenon and iodine, as depicted in Fig. 6, reveal that it takes approximately 9 hours of reactor operation to reach a stable state. From this point forward, xenon/iodine oscillations initiate and persist throughout subsequent cycles. Fig. 7 compares the reactivity contribution of the control rods to the total reactivity with that stemming from coolant temperature feedback and the xenon effect. It is observed that the negative coolant temperature feedback reactivity remains consistent regardless of whether the xenon effect is present or not. In Fig. 9, which presents the total reactivity in the reactor core for both scenarios (with and without the xenon effect), it is evident that the total reactivity offers valuable insights into the reactor's transition from initial criticality to a sub-critical state. This transition is achieved by progressively introducing negative reactivity to reduce the power from 100% to 60%. Subsequently, a different state of criticality is attained and maintained at this power level for 4 hours. To return to nominal power, a positive reactivity is inserted, and the reactor remains critical at this power level until the end of the cycle.

5. Conclusion

A nuclear reactor core was modeled based on the point kinetics equations and one delayed neutron groups. Using the PID controller, the reactor power tracking capability was simulated with a load-following scenario of typical PWR. The proposed model takes into account the impact of feedback from fuel and coolant temperatures on reactor power control. In addition, the xenon concentration effect was also including in the model. Furthermore, the results of the simulations demonstrate the good reactor power tracking by the designed control strategy during a load following scenario. Therefore, it can be concluded that the developed reactor model can be used for further implementation of control strategies (such as Sliding Model Control, LQG/LTR, Fuzzy-PID, Optimal Control, and Model Predictive Control). For the future works, advanced algorithms can be used to optimize PID gains. Moreover, alternative core reactor modeling methods and diverse power control strategies may be considered for implementing power control algorithms in nuclear reactors during load following operations.

References

1. Abdulraheem KK, Korolev S A. Robust optimal-integral sliding mode control for a pressurized water nuclear reactor in load following mode of operation. *Annals of Nuclear Energy.* 2021; 158: 108-288.
2. Li G, Wang X, Liang B, Li X, Zhang B, Zou Y. Modeling and control of nuclear reactor cores for electricity generation: A review of advanced technologies. *Renewable and Sustainable Energy Reviews*. 2016;60:116-128.
3. Dong Z, Cheng Z, Zhu Y, Huang X, Dong Y, Zhang Z. Review on the Recent Progress in Nuclear Plant Dynamical Modeling and Control. *Energies* 2023; 16: 1443.
4. Idrees A, Awais Z, Nadeem S, Rizwan A, Abdus S, Shakeel A. Generating function method for the solution of point reactor kinetic equations. *Progress in Nuclear Energy*.2020; 123 :103-286.
5. Silva MWD, Vilhena MT, Bodmann BEJ, Vasques R. The solution of the neutron point kinetics equation with stochastic extension: an analysis of two moments. *International Nuclear Atlantic Conference – INAC*. 2015.
6. Abdulraheem KK, Korolev SA, Laidani Z. A differentiator based second-order sliding-mode control of a pressurized water nuclear research reactor considering xenon concentration feedback. *Annals of Nuclear Energy* . 2021; 156: 108-193
7. El-Genk MS, Tournier JMP. A point kinetics model for dynamic simulations of next generation nuclear reactor. *Progress in Nuclear Energy* . 2016; 92: 91-103
8. Ismail M, Abulaban D, Genco F, Alkhedher M. Solution of the Reactor Point Neutron Kinetic Equations with Temperature Feedback Control Using MATLAB-Simulink Toolbox. *10th International Conference on Thermal Engineering: Theory and Applications February 26-28*, 2017, Muscat, Oman. 2017.
9. Wright SA. Travis Sanchez. Dynamic Modeling and Control of Nuclear Reactors Coupled to Closed-Loop Brayton Cycle Systems using SIMULINK. *Space Technology and Applications International Forum-STAIF*. 2005
10. Mahendra Kumar JL, Abdul Majeed AP, Zakaria MA, Mohd Razman MA, Khairuddin MI. The Power Level Control of a Pressurised Water Reactor Nuclear Power Plant. InIntelligent Manufacturing and Mechatronics: Proceedings of the 2nd Symposium on Intelligent Manufacturing and Mechatronics–SympoSIMM 2019, 8 July 2019, Melaka, Malaysia 2020 (pp. 451-455). Springer Singapore.
11. Edwards RM, Lee KY, Ray A. Robust optimal control of nuclear reactors and power plants. *Nuclear Technology*. 1992; 98:137-148.
12. Adel BA, Edwards RM, Lee KY. LQG/LTR Robust Control of Nuclear Reactors with Improved Temperature Performance. *IEEE Transactions on Nuclear Science.* December 1992, 39.
13. Dong Z. Nonlinear Adaptive Dynamic Output-Feedback Power-Level Control of Nuclear Heating Reactors. *Science and Technology of Nuclear Installations*. 2013
14. Aab-Alibeik H, Setayeshi S. Improved Temperature Control of a PWR Nuclear Reactor Using an LQG/LTR Based Controller. *IEEE Transactions on Nuclear Science*. 2003; 50:211-218.
15. Ben-Abdennour A., Edwards R.M., Lee K.Y. LQG/LTR robust control of nuclear reactors with improved temperature performance. IEEE *Trans. Nucl. Sci.* 1992;39: 2286-2294
16. Ansarifar GR, Rafiei M. Second-order sliding-mode control for a pressurized water nuclear reactor considering the xenon concentration feedback. *Nucl Eng Techno* . 2015; l47: 94-101
17. Ansarifar GR, Rafiei M. Higher order sliding mode controller design for a research nuclear reactor considering the effect of xenon concentration during load following operation. *Annals of Nuclear Energy*. 2015; 75: 728–735
18. Mehrdad N. Khajavia, Mohammad B. Menhaj AA, Suratgar A. neural network controller for load following operation of nuclear reactors. *Annals of Nuclear Energy*. 2002; 29: 751–760
19. Park MG, Cho NZ. Time-Optimal Control of Nuclear Reactor Power with Adaptive Proportional- Integral -Feed forward Gains. *IEEE Transactions on Nuclear Science*. 1993; 40:266-270.
20. Eliasi H, Menhaj MB, Davilu H. Robust nonlinear model predictive control for a PWR nuclear power plant. *Progress in Nuclear Energy*. 2012; 54: 177-185
21. Mousakazemi SMH, Ayoobian N, Ansarifar GR. Control of the reactor core power in PWR using optimized PID controller with the real-coded GA. *Annals of Nuclear Energy.* 2018; 118: 107–121
22. Liu C, Peng JF, Zhao FY, Li C. Design and optimization of fuzzy-PID controller for the nuclear reactor power control. *Nuclear Engineering and Design* . 2009; 239: 2311–2316
23. Mousakazemi SMH, Ayoobian N, Ansarifar GR. Control of the pressurized water nuclear reactors power using optimized proportionaleintegralederivative controller with particle swarm optimization algorithm. *Nuclear Engineering and Technology*. 2018; 1- 9

24. Rahgoshaya M, Noori-Kalkhoranb O. Calculation of control rod worth and temperature reactivity coefficient of fuel and coolant with burn-up changes for VVRS-2 MWth nuclear reactor. *Nuclear Engineering and Design*. 2013; 256 : 322– 331
25. Eissa M, Naguib M, Badawi A. PWR control rods position monitoring. *Annals of Nuclear Energy* . 2015; 81:106–116.
26. Boustani E, Khoshahval F. Control rods reactivity worth calculation using deterministic and Monte Carlo approaches for an MTR type research reactor. *Iranian Journal of Physics Research*. 2021; 21.
27. Hafez N, Shahbunder H, Amin E, Elfiki SA, Abdel-Latif A. Study on criticality and reactivity coefficients of VVER-1200 reactor. *Progress in Nuclear Energy*. 2021; 131: 103594
28. Louis HK. Neutronic Analysis of the VVER-1200 under Normal Operating Conditions. *Journal of Nuclear and Particle Physics* 2021; 11(3): 53-66

Recommended Citation

Djaroum B, Mohammedi B, Khelil A, Laouar S. Modeling of nuclear reactor core for power control simulation with temperature feedback and xenon concentration effect. *Alger. J. Eng. Technol. 2023*, 08(2). 212-219. https:/dx.doi.org/10.57056/ajet.v8i2.125